Role of Arginine 59 in the γ-Class Carbonic Anhydrases†

Brian C. Tripp,‡,§ Chingkuang Tu,|| and James G. Ferry*,‡

Department of Biochemistry and Molecular Biology, Eberly College of Science, The Pennsylvania State University, University Park, Pennsylvania 16802, and Departments of Pharmacology and Biochemistry, University of Florida College of Medicine, Gainesville, Florida 32610

Received April 16, 2001; Revised Manuscript Received October 23, 2001

ABSTRACT: The functional role of the highly conserved active site Arg 59 in the prototype of the γ-class carbonic anhydrase Cam (carbonic anhydrase from *Methanosarcina thermophila*) was investigated. Variants (R59A, -C, -E, -H, -K, -M, and -Q) were prepared by site-directed mutagenesis and characterized by size exclusion chromatography (SEC), circular dichroism (CD) spectroscopy, and stopped-flow kinetic analyses. CD spectra indicated similar secondary structures for the wild type and the R59A and -K variants, independent of nondenaturing concentrations of guanidine hydrochloride (GdnHCl). SEC indicated that all variants purified as homotrimers like the wild type. SEC also revealed that the R59A and -K variants unfolded at ≥1.5 M GdnHCl, compared to 3.0 M GdnHCl for the wild type. These results indicate that Arg 59 contributes to the thermodynamic stability of the Cam trimer. The R59K variant had k_{cat} and k_{cat}/K_m values that were 8 and 5% of the wild-type values, respectively, while all other variants had k_{cat} and k_{cat}/K_m values 10−100-fold lower than those of the wild type. The R59A, -C, -E, -M, and -Q variants exhibited 4−63-fold increases in k_{cat} and 9−120-fold increases in k_{cat}/K_m upon addition of 100 mM GdnHCl, with the largest increases observed for the R59A variant, which was comparable to the R59K variant. The kinetic results indicate that a positive charge at position 59 is essential for the CO_2 hydration step of the overall catalytic mechanism.

There are three independently evolved classes of carbonic anhydrases (α, β, and γ) known which all catalyze the same CO_2 hydration reaction (eq 1).

$$CO_2 + H_2O \rightleftharpoons H^+ + HCO_3^- \quad (1)$$

The carbonic anhydrase (Cam)[1] from the archaeon *Methanosarcina thermophila* is the prototype and only member of the γ-class that has been structurally and kinetically characterized. Cam is a homotrimeric zinc enzyme primarily composed of a left-handed β-helical fold, the sequence of which is significantly similar to that of a larger family of left-handed β-helical acyltransferases (*1*). The active site of Cam is located at the interface between adjacent monomers and contains a zinc coordinated by three histidine residues, two of which are donated by one monomer (His 81-A and His 122-A), while the third histidine is donated from an adjacent monomer (His 117-B). Inspection of the crystal structure indicates an active site Arg 59 that is hypothesized to be important in subunit association (*2*, *3*). The Arg 59 guanido side chain forms electrostatic interactions with negatively charged carboxylate side chains of Asp 61-A from the same monomer and Asp 76-B from the adjoining monomer. Thus, Arg 59 has been proposed to fulfill an important "salt-bridge" structural role in stabilization of the Cam trimer (*2*). However, other features of the crystal structure also suggest a potential role for Arg 59 in catalysis. The Arg 59 side chain guanido group is partially solvent-exposed and 6 Å from the metal ion (*2*, *3*). Preliminary crystallographic evidence in a more recent high-resolution crystal structure of Cam cocrystallized with bicarbonate indicated an oblong nonaqueous electron density adjacent to Arg 59 which could be tentatively modeled as low-occupancy bicarbonate binding (T. Iverson, personal communication). There are also many examples of arginine residues that bind to substrate carboxylate groups in enzyme active sites, including carboxypeptidase A (*4*−*6*) and other enzymes (*7*−*19*).

The functional roles of most active site residues in α-class carbonic anhydrases are well-defined; however, no functional role has been assigned for arginine (*20*). The relatively slow α-class carbonic anhydrase III has a nonconserved, solvent-exposed arginine residue located approximately 9 Å from the active site zinc ion (*21*). This arginine can be substituted with asparagine to obtain enhanced rates of CO_2 hydration (*22*), indicating that it is not essential for catalysis. In contrast

† This work was supported by grants from the National Institutes of Health to J.G.F. (GM44661) and D. N. Silverman (GM25154). B.C.T. was supported by a National Science Foundation-Research Training Grant Fellowship (DBI-9602232).

* To whom correspondence should be addressed. Phone: (814) 863-5721. Fax: (814) 863-6217. E-mail: jgf3@psu.edu.

‡ The Pennsylvania State University.

§ Current address: Departments of Biological Sciences and Chemistry, College of Arts and Sciences, Western Michigan University, Kalamazoo, MI 49008.

|| University of Florida College of Medicine.

[1] Abbreviations: Cam, *M. thermophila* carbonic anhydrase produced in *Escherichia coli*; CD, circular dichroism; SEC, size exclusion chromatography; A_{600}, absorbance at 600 nm; IPTG, isopropyl thiogalactopyranoside; A_{280}, absorbance at 280 nm; GdnHCl, guanidine hydrochloride; MOPS, 2-(*N*-morpholino)propanesulfonic acid; HIC, hydrophobic interaction chromatography; MES, 2-(*N*-morpholino)-ethanesulfonic acid; TAPS, *N*-tris(hydroxymethyl)methyl-3-aminopropanesulfonic acid.

10.1021/bi010768b CCC: $22.00
Published on Web 12/13/2001

to α-class carbonic anhydrases, the importance and function of most Cam active site residues are unknown. Other than the presence of three histidines coordinating the zinc ion, there are few obvious similarities between the α- and γ-class active sites. Two active site glutamate residues (Glu 62 and Glu 84) have been shown to be important for catalysis and proton transport in Cam (*23*), while other residues remain to be investigated. Arg 59 in Cam is conserved in all 35 Cam homologues identified in the databases (*24*). Several recent plant and prokaryotic *β*-class carbonic anhydrase crystal structures show a conserved, active site arginine, although no role has been proposed for this residue (*25*−*27*). The influence of Arg 59 on the trimer stability and catalysis of Cam was investigated by CD spectroscopy, SEC, and kinetic analysis of Arg 59 substitution variants. Here, we demonstrate that Arg 59 contributes to the thermodynamic stability of the Cam trimer, addressing the previously hypothesized salt-bridge role in stabilizing monomer interactions. We also present evidence that the positive charge at the position of this residue is essential for the CO_2 hydration step of catalysis.

MATERIALS AND METHODS

Mutagenesis and Expression. A plasmid encoding the sequence of a putative mature or soluble form of Cam, termed pCAM-AC, was used as the starting plasmid for all site-directed mutagenesis experiments. This is a modified version of plasmid pBA1416NB (*28*) that contains two unique *Ban*II and *Bsr*GI restriction sites (*23*), and is derived from plasmid pT7-7 (*29*). The encoded form of Cam has a 34-amino acid deletion from the N-terminal sequence, which has properties characteristic of a secretory signal peptide leader sequence. Mutations were introduced at amino acid position 59 by use of the QuikChange site-directed mutagenesis kit (Stratagene, La Jolla, CA). Mutations were confirmed by DNA sequencing of the entire region encoding the Cam protein in the plasmids. *Escherichia coli* strain BL21(DE3) or BL21(DE3) Gold was transformed with pCAM-AC or derivative mutated plasmids, and used to inoculate Luria-Bertani broth containing 100 μg/mL ampicillin and 500 μM $ZnSO_4$. Cells were grown at 37 °C to an A_{600} of 0.4−0.8, and induced to overproduce Cam variants by addition of IPTG to a final concentration of 0.8 mM, followed by continued growth at 37 °C for 3 h. Cells were then harvested by centrifugation and stored frozen at −80 °C until lysis was performed. Molecular biology procedures were performed according to Sambrook et al. (*30*).

Protein Purification. All chromatography columns and resins were from Amersham Pharmacia Biotech (Piscataway, NJ). Cells were lysed by resuspension in 50 mM MOPS buffer (pH 7.5) to an A_{600} of 2−10, followed by two passes through a chilled French press at a pressure of 1000 lb/in.^{2} (1 lb/in.^{2} = 6.9 kPa). The cell lysate was centrifuged at 20000−50000*g* for 20 min, followed by filtration of the supernatant through a 0.45 μm filter. The soluble cell extract solution was then loaded onto a Q-Sepharose fast flow anion exchange column and washed with 2 column volumes of 50 mM MOPS buffer (pH 7.5). A gradient of 0 to 1.0 M NaCl was then applied over 10 bed volumes to the column to elute the Cam fractions, which typically eluted at a NaCl concentration of 0.5 M. The Cam fractions were then pooled and diluted 1-fold with 3.0 M $(NH_4)_2SO_4$ previously equilibrated with Chelex resin (Bio-Rad, Hercules, CA) to remove contaminating iron, to give a final $(NH_4)_2SO_4$ concentration of 1.5 M. This solution was then loaded onto a Phenyl-Sepharose high-performance HIC column previously equilibrated with 50 mM MOPS (pH 7.5) containing 1.5 M $(NH_4)_2SO_4$. The column was washed with several bed volumes of equilibration buffer, and then Cam was eluted by applying a decreasing gradient of buffer containing 1.5 to 0 M $(NH_4)_2SO_4$. Cam fractions were then pooled, dialyzed against 50 mM MOPS buffer (pH 7.5), aliquoted and frozen in liquid nitrogen, and stored at −80 °C until further use. Freezing and thawing resulted in formation of aggregates of the purified R59E, -M, and -Q variants, as determined by SEC. Thus, following HIC purification, these three variants were immediately exchanged into 50 mM MOPS buffer (pH 7.5) with a PD-10 desalting column and the kinetics constants determined. Concentrations of the purified wild type and all Arg 59 variants were determined by measuring the A_{280} values of protein solutions using a theoretical molar absorbance value of 15 990 M^{-1} cm^{-1} and a computed monomer molecular mass of 22 873 Da.

Size Exclusion Chromatography. A Superose-12 high-resolution SEC column was equilibrated with 50 mM MOPS buffer (pH 7.5) containing 50 mM Na_2SO_4. A volume of 200 μL of each Cam variant at a concentration of 20 μM was injected onto the column and eluted at a flow rate of 0.5 mL/min. Eluting protein was detected by measuring the absorbance at 280 nm. Molecular masses were estimated from a calibration curve established from the retention times of purified bovine serum albumin, cytochrome *c*, hen lysozyme, bovine carbonic anhydrase II, alcohol dehydrogenase, and *β*-amylase proteins, and the column void volume was determined with blue dextran, all obtained from Sigma Chemical Co. (St. Louis, MO). For SEC studies with GdnHCl, each protein was incubated for 2 h at 25 °C in 50 mM MOPS buffer (pH 7.5) with the indicated concentration of GdnHCl, and the ionic strength was adjusted to a minimum of 0.2 M with Na_2SO_4. A volume of 200 μL of each sample at a concentration of 20 μM was then loaded onto and eluted from a SEC column pre-equilibrated with the same buffer.

Circular Dichroism Spectroscopy. CD spectra were collected on an AVIV (Lakewood, NJ) model 62 DS circular dichroism spectrophotometer at 25 °C, using a 2 mm path length quartz cuvette, at a protein monomer concentration of 10 μM, in 50 mM MOPS buffer (pH 7.5) containing either 50 mM Na_2SO_4 or 100 mM GdnHCl and 16.7 mM Na_2SO_4. Protein solutions were scanned over the wavelength range of 200−260 nm, using a bandwidth of 2.0 nm, with an averaging time of 5 s for each data point.

Steady-State Kinetic Measurements. Wild-type Cam and variants of interest were assayed for carbonic anhydrase activity by the method of Khalifah (*31*), using a KinTek model SF-2001 stopped-flow instrument (KinTek Corp., Austin, TX). Enzyme monomer concentrations ranged from 200 nM to 20 μM. Buffer−indicator dye pairs that were used were as follows: at pH 6.0−6.5, MES and chlorophenol red measured at 574 nm; at pH 7.0−7.5, MOPS and 4-nitrophenol measured at 400 nm; and at pH 7.7−9.1, TAPS and *m*-cresol purple measured at 578 nm. MOPS, MES, and TAPS buffer concentrations were always 50 mM, and the ionic strength of each buffer solution was adjusted to a

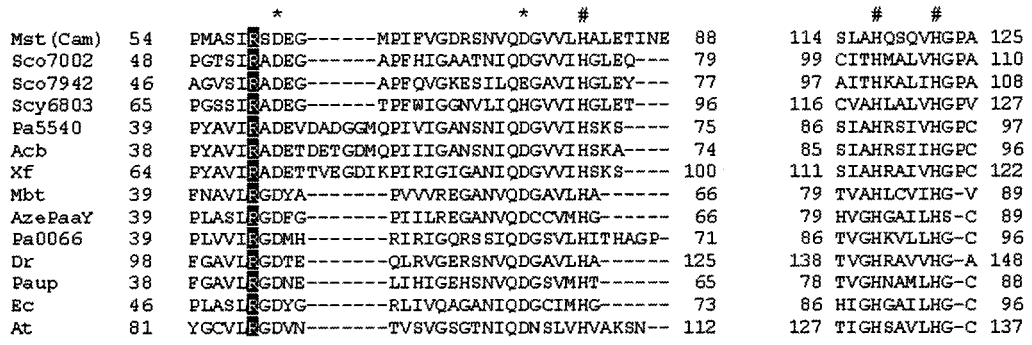

FIGURE 1: Partial sequence alignment of Cam with representative Cam homologues from diverse organisms. The conserved arginine (Arg 59 in Cam) is shown in reverse boldface. Asterisks (*) denote conserved Asp 61 and Asp 76 residues that interact with Arg 59. Pound symbols (#) denote the three conserved histidines (His 81, His 117, and His 122) that coordinate the active site transition metal ion. Legend (GenBank accession numbers in parentheses): Mst(Cam), *M. thermophila* γ-class carbonic anhydrase (1827571); Sco7002, *Synechococcus* PCC7002 carbon dioxide-concentrating mechanism protein (2331052); Sco7942, *Synechococcus* PCC7942 carbon dioxide-concentrating mechanism protein CcmM (416775); Scy6803, *Synechocystis* sp. strain PCC 6803 carbon dioxide-concentrating mechanism protein CcmM (7469276); Pa5540, *Pseudomonas aeruginosa* strain PAO1 hypothetical protein PA5540 (11350492); Acb, *Acinetobacter* sp. ADP1 carbonic anhydrase homologue (6127222); Xf, *Xylella fastidiosa* strain 9a5c carbonic anhydrase XF2095 (11360537); Mbt, *Mycobacterium tuberculosis* hypothetical protein Rv3525c (7447198); AzePaay, *Azoarcus evansii* gene product PaaY involved in aerobic phenyl acetate metabolism (11072184); Pa0066, *P. aeruginosa* strain PAO1 conserved hypothetical protein PA0066 (11347610); Dr, *Deinococcus radiodurans* ferripyochelin binding protein (7471892); Paup, *P. aeruginosa* unknown protein (151224); Ec, *E. coli* O157:H7 possible synthesis of cofactor for carnitine racemase and dehydratase (12512722); and At, *Arabidopsis thaliana* unknown protein (9795586).

minimum of 0.2 M with Na_2SO_4. Each rescue agent (100 mM) was used in comparative assays involving chemical rescue of R59A and R59C variants by various amino and guanido compounds, and the initial pH of all rescue assay buffers was 7.5. The hydrochloride salt of guanidine, the chloride salt of methylguanidine, and the sulfate salt of ethylguanidine were used in these rescue experiments. GdnHCl (100 mM) was present in the buffers used to measure the pH-dependent CO_2 hydration rate of the R59A variant. Final pH indicator concentrations ranged from 2 to 100 μM. Saturated solutions of CO_2 (32.9 mM in H_2O) were prepared by bubbling CO_2 gas into deionized water at 25 °C. The experimental CO_2 concentrations were varied from 4.7 to 24 mM in H_2O. Only the initial 5−10% of the data was used for kinetic analysis, using the average of 5−10 reaction traces per experiment. The initial rate data were fit to the Michaelis−Menten equation to obtain experimental values for k_{cat} and K_m. The pH-independent values of k_{cat} and pK_a for CO_2 hydration of the wild type and the R59A and -K variants were determined by fitting the experimental pH-dependent Michaelis−Menten parameter k_{cat} to eq 2.

$$k_{cat}^{obs} = k_{cat}/(1 + 10^{pK_a - pH}) \quad (2)$$

The pH-independent values for k_{cat}/K_m^{I}, k_{cat}/K_m^{II}, pK_a^{I}, and pK_a^{II} for CO_2 hydration of R59A and -K variants were determined by fitting the pH-dependent Michaelis−Menten parameter k_{cat}/K_m to eq 3.

$$k_{cat}/K_m^{obs} = [(k_{cat}/K_m^{I}) \times 10^{pK_a^{II} - pH} + k_{cat}/K_m^{II}]/ (1 + 10^{pK_a^{II} + pK_a^{I} - 2pH} + 10^{pK_a^{I} - pH} + 10^{pK_a^{II} - pH}) \quad (3)$$

All data fits were performed with the Kaleidagraph software package (Synergy Software, Reading, PA).

^{18}O Exchange Experiments. The R59A variant was characterized with respect to its ability to catalyze the exchange of ^{18}O between water and CO_2 at chemical equilibrium as a function of GdnHCl concentration, using pH 7.9, 100 mM HEPES buffer at 0−250 mM GdnHCl. This method has been previously described in detail (*32*, *33*). An Extrel EXM-200 mass spectrometer with a membrane-inlet probe was used to monitor the isotopic content of CO_2. The interconversion of ^{18}O-labeled bicarbonate to ^{18}O-labeled H_2O via a CO_2 intermediate is described by eqs 4 and 5.

$$HCOO^{18}O^- + EZnH_2O \rightleftharpoons EZnHCOO^{18}O^- + H_2O \rightleftharpoons COO + EZn^{18}OH^- + H_2O \quad (4)$$

$$EZn^{18}OH^- + BH^+ + H_2O \rightleftharpoons EZnH_2{}^{18}O + B + H_2O \rightleftharpoons EZnH_2O + H_2{}^{18}O + B \quad (5)$$

The kinetic equations for the redistribution of ^{18}O from the $CO_2-HCO_3^-$ system to water were solved to obtain R_1, the rate of exchange of CO_2 and HCO_3^- at chemical equilibrium, and R_{H_2O}, the rate of release of ^{18}O-labeled water from the enzyme (*32*).

RESULTS

Initial Characterization of Arg 59 Variants. At least 35 deduced prokaryotic protein sequences (30 bacterial, 5 archaeal) and one eukaryotic sequence, which was significantly identical to Cam, have been identified in the databases (*24*). Cam active site residues Gln 75 and Asp 76 are highly conserved, whereas Arg 59, Asp 61, and the ligands to the active site zinc (His 81, His 117, and His 122) are perfectly conserved among all 35 homologues. A partial alignment of Cam with representative Cam homologues is shown in Figure 1. Cam Arg 59 is indirectly hydrogen-bonded to the active site zinc through a network that includes Asp 61, Asp 76, His 81, and His 117 (Figure 2). The strict conservation of Arg 59 in Cam homologues and the proximity to the active site zinc in Cam suggest this residue may play a role in catalysis in addition to the previously hypothesized role in subunit interactions contributing to trimer stability (*2*). Thus,

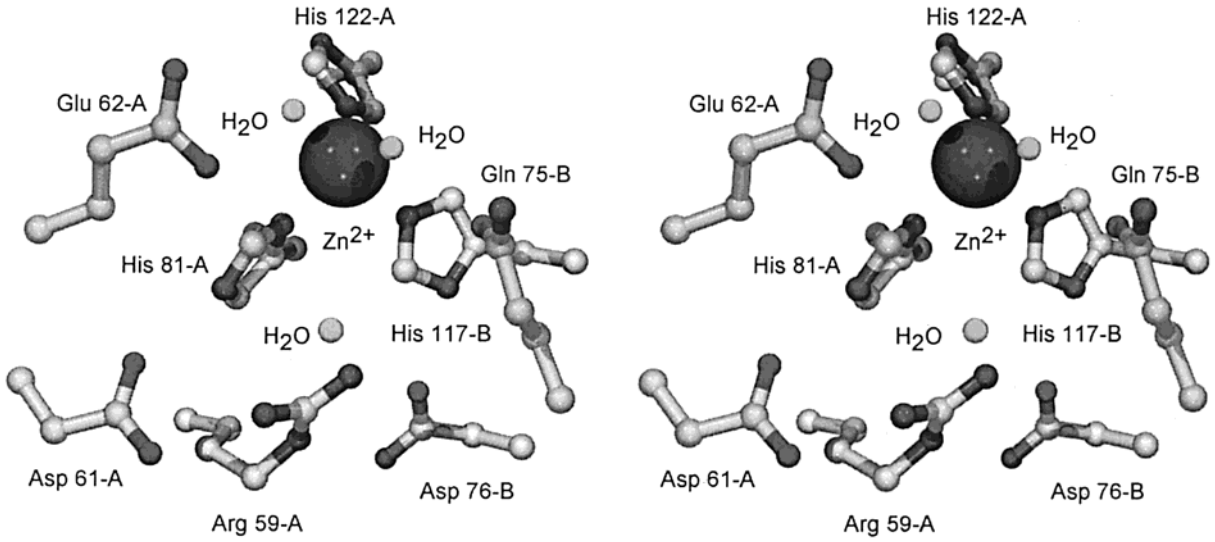

FIGURE 2: Stereoview of Arg 59, neighboring residues, and water molecules in the active site of Cam. The image was produced using SwissPDBviewer software (*48*) with the Protein Data Bank structure 1QRG and rendered with the POV-Ray software package.

Cam variants R59A, -C, -E, -H, -K, -M, and -Q were obtained by site-directed mutagenesis to provide substitutions at position 59 with different side chain size, polarity, or charge. All seven variants were expressed in a soluble form in *E. coli*, with final yields of 20−50 mg of the purified variant/L of cell culture, similar to the yield of the wild type. These variants also exhibited elution profiles similar to that of the wild type during the Q-Sepharose anion exchange and HIC purification steps. SDS−PAGE indicated a purity of at least 95% for all the variants. The molecular mass of each variant was characterized by SEC with a Superose 12 column immediately following purification. Each freshly purified variant eluted as a single symmetric peak with a native molecular mass of approximately 80 kDa, identical to that of the trimeric wild type.

Role of Arg 59 in Stabilization of the Cam Trimer. SEC indicated that the freshly purified R59A, -C, -H, and -K variants remained trimeric in 0 M, 100 mM, and 1.0 M GdnHCl. Thus, these four variants did not dissociate into monomers under the initial (350 mM) and final (100 mM) GdnHCl conditions used in chemical rescue stopped-flow experiments discussed below. Freshly purified wild type and R59A, -C, -H, and -K variants remained trimeric when stored for 1 week at 4 °C. Conversely, SEC showed that the freshly purified trimeric R59E, -M, and -Q variants converted to multimeric mixtures ranging in molecular mass from 30 to 200 kDa within 24 h when stored in solution in MOPS buffer at 4 °C; thus, the association state of the freshly purified trimeric R59E, -M, and -Q variants in 100 mM or 1.0 M GdnHCl was not determined. SEC indicated that the freshly purified R59A, -C, -H, and -K variants remained trimeric after one freeze−thaw cycle while the R59E, -M, and -Q variants were converted to a mixture of monomers, trimers, hexamers, and multimeric aggregates larger than 2×10^6 Da. These multimeric forms of the R59E, -M, and -Q variants obtained after freezing and thawing were insoluble in 1.5 M $(NH_4)_2SO_4$, unlike the wild type and freshly purified trimeric forms of all seven Arg 59 variants.

The extent to which Arg 59 contributes to the stability of the Cam trimer was investigated in further detail by gauging the effect of increasing GdnHCl concentrations on the

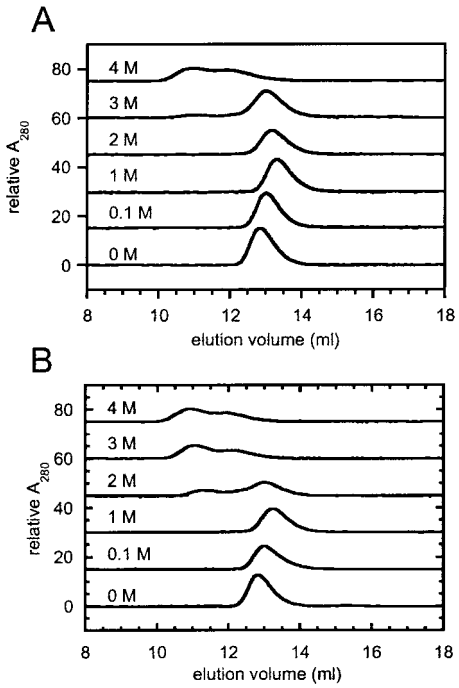

FIGURE 3: Size exclusion chromatography (SEC) elution profiles of wild type Cam and the R59A variant as a function of the guanidine hydrochloride concentration: (A) wild type Cam and (B) R59A Cam. Each protein was equilibrated with buffer containing the indicated concentration of guanidine hydrochloride for 2 h prior to SEC (see Materials and Methods).

molecular mass of the wild type compared to the masses of the R59A and -K variants as monitored by SEC. Wild-type Cam eluted as a single symmetric peak indicative of an ∼80 kDa trimer at ∼12.8−13.2 mL in 0−3 M GdnHCl (Figure 3A), while the R59A variant eluted as a trimer in 0−1.5 M GdnHCl (Figure 3B). Some minor variation was apparent in both the wild-type and variant trimer elution volumes. This variation resulted from changes in the porosity of the SEC resin associated with the high ionic strength effects at ≥1 M GdnHCl, and does not reflect the dissociation of the trimer into monomers. Metal-free forms of the wild type and the R59A variant separate into a mixture of monomers and trimers which elute as two separate peaks, with the easily

Table 1: Apparent pH-Dependent Stopped-Flow Michaelis−Menten Kinetic Parameters for Chemical Rescue of Cam Variants R59A and R59C by Guanido Compounds, Urea, Imidazole, and Ethylamine

variant[a]	rescue agent[b]	k_{cat} ($\times 10^{-3}$ s^{-1})	K_m ($\times 10^3$ M)	k_{cat}/K_m ($\times 10^{-5}$ M^{-1} s^{-1})
R59A	none	0.070 ± 0.010	15.7 ± 4.6	0.045 ± 0.020
	guanidine (50 mM)	2.71 ± 0.10	14.5 ± 1.1	1.87 ± 0.22
	guanidine (100 mM)	3.27 ± 0.29	17.1 ± 2.9	1.92 ± 0.49
	guanidine (150 mM)	2.25 ± 0.97	11.7 ± 1.1	1.93 ± 0.27
	methylguanidine	5.69 ± 0.29	12.2 ± 1.37	4.68 ± 0.77
	ethylguanidine	7.14 ± 0.53	16.2 ± 2.36	4.41 ± 0.98
	aminoguanidine	0.35 ± 0.02	9.45 ± 1.27	0.37 ± 0.070
	ethylamine	0.16 ± 0.02	25.4 ± 5.34	0.064 ± 0.022
	imidazole	0.11 ± 0.04	34.0 ± 20.3	0.031 ± 0.031
	urea	0.028 ± 0.010	26.2 ± 14.1	0.011 ± 0.010
	1,3-diaminoguanidine	0.012 ± 0.024	12.8 ± 50.5	0.010 ± 0.056
R59C	none	0.52 ± 0.02	34.2 ± 1.9	0.15 ± 0.014
	guanidine	2.17 ± 0.15	13.6 ± 2.0	1.59 ± 0.34
	methylguanidine	0.99 ± 0.07	17.3 ± 2.2	0.57 ± 0.11
	ethylguanidine	0.31 ± 0.03	6.5 ± 1.7	0.48 ± 0.16
	aminoguanidine	0.32 ± 0.31	47.6 ± 62.4	0.068 ± 0.154

[a] Experimental conditions are described in Materials and Methods. [b] The concentration of each rescue agent was 100 mM except where indicated in parentheses.

distinguished ~30 kDa monomer species eluting 1.1 mL after the trimer species (data not shown). Thus, the SEC data indicate that the wild type and the R59A variant did not dissociate into monomers or unfold until >3 and >1.5 M GdnHCl, respectively.

Proteins unfolded by high concentrations of chemical denaturants such as GdnHCl and urea have detectably larger hydrodynamic radii than their native conformations (*34*−*36*). The different random-coil forms of an unfolded protein can be resolved from well-folded globular conformations of the same protein by SEC with a Superose 12 column, which is not significantly affected by the presence of high concentrations of chemical denaturants such as GdnHCl or urea (*34*). In this type of experiment, larger unfolded forms of proteins elute earlier from the SEC column than the smaller folded forms. The wild type and the R59A variant eluted as significantly larger molecular mass species at >3.0 and >1.5 M GdnHCl, indicative of unfolded protein at these higher GdnHCl concentrations (Figure 3). The R59K variant also eluted as a trimer in 0−1.5 M GdnHCl, followed by apparent unfolding at >2 M GdnHCl (data not shown).

Kinetic Characterization of Arg 59 Variants. The R59A, -C, -E, -H, -K, -M, and -Q variants were kinetically characterized by steady-state stopped-flow measurements (Table 1). Only the conservative R59K variant exhibited significant activity in the absence of GdnHCl with k_{cat} and k_{cat}/K_m values that were 7.5 and 4.9% of that of the wild type, respectively. The R59A, -C, -E, -H, -M, and -Q variants had k_{cat} and k_{cat}/K_m values that were <1% of those of the wild type.

CD spectra were compared for the trimeric wild type and the R59A and -K variants to rule out changes in secondary structure that might contribute to the loss of activity. The mean residue ellipticities at a wavelength of 222 nm (MRE_{222}) for the wild type and the R59A and -K variants are listed in Table 2. The CD spectra for the wild type and the R59A and -K variants were very similar in shape (data not shown), with only a 0.93% difference in MRE_{222} for the R59A variant and the wild type and a 3.1% difference in MRE_{222} between the R59K variant and wild type. The wild type exhibited a 1.8% lower (more negative) MRE_{222} in the presence of GdnHCl, while the R59A and -K variants exhibited 5.4 and 6.3% higher (less negative) MRE_{222} values, respectively, in the presence of 100 mM GdnHCl (Table 2). These results indicate that the trimeric R59A and -K variants have secondary structures similar to that of the wild type, and that these secondary structures are not significantly altered by the presence of 100 mM GdnHCl.

Table 2: Mean Residue Ellipticities for Wild-Type Cam and Arginine 59 Cam Variants

	MRE_{222}[a] (deg cm^{-2} $dmol^{-1}$)	
	without GdnHCl[b]	with GdnHCl[c]
wild type	−7981.2	−8125.8
R59A	−7907.3	−7484.1
R59K	−8227.8	−7708.0

[a] MRE_{222} (mean residue ellipticity at 222 nm) determined by circular dichroism spectroscopy as described in Materials and Methods using 3.3 μM Cam trimer. [b] In 50 mM MOPS (pH 7.5) and 50 mM Na_2SO_4. [c] In 50 mM MOPS (pH 7.5), 100 mM GdnHCl, and 16.7 mM Na_2SO_4.

Chemical Rescue of Arg 59 Variants. There is precedent for chemical rescue of catalytic activity of arginine deletion variants by guanido compounds (*37*−*41*). Thus, an initial stopped-flow kinetic experiment was performed to determine the catalytic activity of the R59A variant in the presence and absence of nondenaturing concentrations of GdnHCl. The presence of GdnHCl significantly increased the k_{cat} and k_{cat}/K_m values of the R59A variant. The highest k_{cat} and k_{cat}/K_m values for the R59A variant were obtained with 100 mM GdnHCl (Table 1); thus, all further chemical rescue stopped-flow experiments were performed with 100 mM rescue agents.

Other compounds were screened for their relative abilities to rescue k_{cat} and k_{cat}/K_m of the R59A variant (Table 1). The ethyl-, methyl-, and aminoguanidine derivatives increased the k_{cat} and k_{cat}/K_m values. 1,3-Diaminoguanidine, uncharged urea, and the weak base imidazole failed to significantly rescue the R59A variant. The relative order of rescued k_{cat} and k_{cat}/K_m values for the R59A variant was as follows: ethylguanidine > methylguanidine > guanidine ≫ aminoguanidine > ethylamine. The R59C variant exhibited the second highest k_{cat} and k_{cat}/K_m values of all the Arg 59

Table 3: Apparent pH-Dependent Stopped-Flow Michaelis−Menten Kinetic Parameters for Wild-Type Cam and Cam Variants in the Absence and Presence of Guanidine Hydrochloride

	k_{cat} ($\times 10^{-3}$ s^{-1})		K_m ($\times 10^3$ M)		k_{cat}/K_m ($\times 10^{-5}$ M^{-1} s^{-1})	
variant	without GdnHCl[a]	with GdnHCl[b]	without GdnHCl	with GdnHCl	without GdnHCl	with GdnHCl
wild type	62.9 ± 3.7	29.2 ± 4.0	21.8 ± 2.2	16.7 ± 4.4	28.9 ± 4.7	17.5 ± 7.1
R59A	0.070 ± 0.010	3.27 ± 0.29	15.7 ± 4.6	17.1 ± 2.9	0.045 ± 0.020	1.92 ± 0.49
R59C	0.52 ± 0.02	2.17 ± 0.15	34.2 ± 1.9	13.6 ± 2.0	0.15 ± 0.014	1.59 ± 0.34
R59E	0.019 ± 0.067	0.067 ± 0.019	51.4 ± 239	19.3 ± 10.2	0.004 ± 0.031	0.035 ± 0.028
R59H	0.042 ± 0.014	0.012 ± 0.006	25.0 ± 14.0	6.09 ± 8.92	0.017 ± 0.015	0.020 ± 0.038
R59K	4.72 ± 0.21	2.74 ± 0.18	33.4 ± 2.24	19.1 ± 2.30	1.41 ± 0.16	1.43 ± 0.27
R59M	0.013 ± 0.033	0.159 ± 0.011	43.3 ± 152	16.3 ± 2.3	0.003 ± 0.018	0.098 ± 0.021
R59Q	0.010 ± 0.014	0.627 ± 0.038	33.9 ± 71.8	17.3 ± 2.0	0.003 ± 0.011	0.363 ± 0.063

[a] Experimental conditions described in Materials and Methods. [b] In 100 mM GdnHCl.

variants rescued with GdnHCl (Table 3). Thus, a similar comparative rescue study was also performed with the R59C variant and the four guanido compounds that were most effective in rescuing the R59A variant (Table 1). Aminoguanidine failed to rescue the R59C variant, and the order of relative effectiveness of chemical rescue was reversed relative to the R59A variant for guanidine, methylguanidine, and ethylguanidine.

Steady-state stopped-flow kinetic analyses of the wild type and the R59C, -E, -H, -K, -M, and -Q variants were determined in the presence of nondenaturing 100 mM GdnHCl to investigate guanidine rescue of catalysis (Table 3) as a function of side chain substitution. The initial rescue studies with the R59A and R59C variants did not indicate a clearly superior guanido compound, as guanidine was more effective at rescuing the R59C variant while ethylguanidine yielded the greatest increase and largest rescued value of k_{cat} and k_{cat}/K_m for the R59A variant. Thus, all further rescue experiments were performed using GdnHCl, based on purity and cost relative to the other rescue agents that were tested.

The K_m values of the wild type and all the variants changed little in the presence of 100 mM GdnHCl (Table 3). The wild-type k_{cat} and k_{cat}/K_m values decreased 54 and 39%, respectively, in the presence of GdnHCl. In contrast to the wild type, the R59A, -C, -E, -M, and -Q variants exhibited significant increases in k_{cat} and k_{cat}/K_m values in the presence of GdnHCl. Rescue of the R59A variant showed the highest k_{cat} and k_{cat}/K_m values that were 11.2 and 11.0% of the wild-type values, respectively, also obtained in the presence of GdnHCl. The k_{cat} and k_{cat}/K_m values for the R59A, -C, -E, -M, and -Q variants exhibited an inverse dependence on the substituted side chain volume when rescued by GdnHCl (Figure 4). The changes in the R59A variant k_{cat} and k_{cat}/K_m values were similar; however, the R59C, -E, -M, and -Q variants exhibited greater increases in k_{cat}/K_m than for k_{cat} in GdnHCl (Table 4).

The rate of ^{18}O-labeled H_2O exchange as a function of GdnHCl concentration was also measured for the R59A variant (Figure 5). The rate of interconversion of CO_2 and HCO_3^- at chemical equilibrium by the R59A variant exhibited a strong hyperbolic concentration dependence on GdnHCl as reflected in the R_1/[E] parameter, with maximum values observed at 150−250 mM GdnHCl. These data were fit to a form of the Michaelis−Menten equation given by $R_1/[E] = k_{cat}^{ex}[GdnHCl]/(K_{eff}^{GdnHCl} + [GdnHCl])$, which yielded fitted values for k_{cat}^{ex} of 511 ± 13 s^{-1} and K_{eff}^{GdnHCl} of 35.3 ± 2.4 mM GdnHCl. The rate of release of ^{18}O-labeled H_2O, R_{H_2O}, exhibited a minimal dependence on the GdnHCl concentration (data not shown).

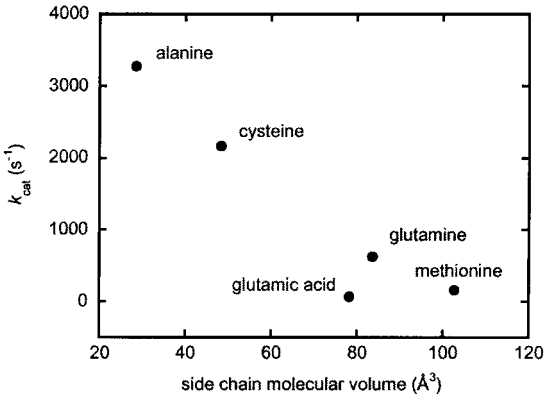

FIGURE 4: Plot of guanidine-rescued k_{cat} values as a function of amino acid side chain volume for the R59A, -C, -E, -M, and -Q variants. Assay conditions: 50 mM MOPS (pH 7.5) containing 16.7 mM Na_2SO_4 and 100 mM GdnHCl buffer. Amino acid side chain molecular volumes were estimated by subtracting the published glycine volume (60.1 Å^3) from other published amino acid volumes (*49*).

Table 4: Effect of Guanidine Hydrochloride on Michaelis−Menten Kinetic Parameters

	ratio of change in k_{cat}[a]	ratio of change in K_m[a]	ratio of change in k_{cat}/K_m[a]
wild type	0.46	0.77	0.61
R59A	46.7	1.09	42.7
R59C	4.17	0.40	10.6
R59E	3.53	0.38	8.75
R59H	0.29	0.24	1.18
R59K	0.58	0.57	1.01
R59M	12.2	0.38	32.7
R59Q	62.7	0.51	121.0

[a] Values are derived from parameters in Table 3. Ratio of the increase or decrease in k_{cat}, K_m, or k_{cat}/K_m in the presence of 100 mM GdnHCl relative to the parameter value in the absence of GdnHCl.

The activities of the R59K variant and the GdnHCl-rescued R59A variant were high enough to measure the steady-state kinetic parameters by the stopped-flow method as a function of pH over the range of 6.0−9.3 (Figure 6). The k_{cat} and k_{cat}/K_m values of the R59K variant and the R59A variant in the presence of GdnHCl were both approximately 10-fold lower than the reported wild-type values (*23*, *42*) over the entire experimental pH range. The k_{cat}/K_m values followed the same general trend as that reported for the wild type (*23*, *42*), increasing from pH 6 to 9. The k_{cat} values of both variants also follow the same trend as that of the wild type at lower pH values, increasing from pH 6−7, and exhibited

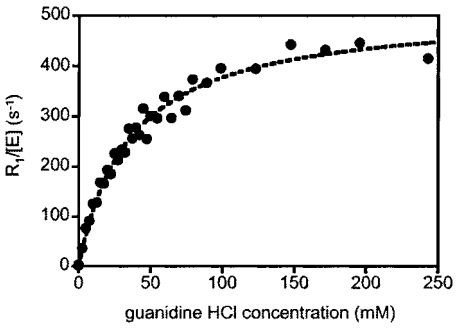

FIGURE 5: Effect of the guanidine hydrochloride concentration on the rate of ^{18}O exchange by the R59A variant.

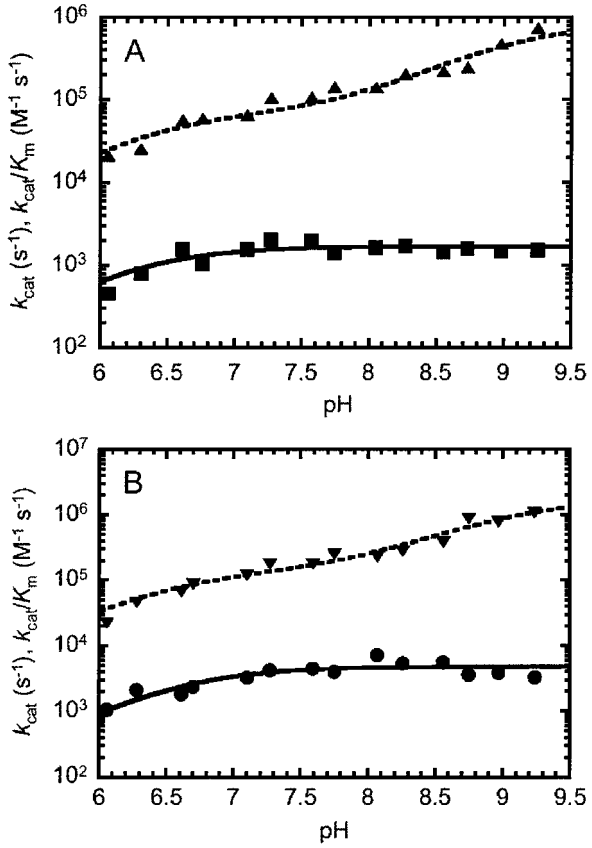

FIGURE 6: pH-dependent steady-state kinetic parameters for the R59K Cam variant and the R59A Cam variant in the presence of 100 mM guanidine hydrochloride. (A) (■) k_{cat} of R59A with 100 mM guanidine hydrochloride and (▲) k_{cat}/K_m of R59A with 100 mM guanidine hydrochloride. (B) (●) k_{cat} of R59K and (▼) k_{cat}/K_m of R59K.

little increase over the pH range of 7−9. The k_{cat} data for both variants were fitted to a single-pK_a model (eq 2), while the k_{cat}/K_m data were fitted to a two-pK_a model (eq 3) (Table 5). The pH-independent k_{cat} value for the R59A variant was slightly lower than the value for the R59K variant; however, both values are in the range reported for the wild type. The fit of the R59A variant k_{cat}/K_m data yielded pK_a^I and pK_a^{II} values similar to those of the R59K variant. The k_{cat}/K_m pH-independent pK_a values of the R59A and -K variants were also similar to that of the wild type; however, the error associated with the pK_a^I values precluded comparison with the wild type. The steady-state kinetic parameters were also determined for the R59A variant in the absence of GdnHCl at pH 6.6, 7.6, and 8.6 (data not shown). The same general trend of increasing k_{cat} and k_{cat}/K_m values with increasing pH was also observed for the R59A variant in the absence of GdnHCl, although the large error inherent in the k_{cat} and k_{cat}/K_m values precluded accurate determination of pK_a values, even at high enzyme concentrations.

Table 5: pH-Independent Michaelis−Menten Kinetic Parameters Derived from the pH Dependence of CO_2 Hydration Catalyzed by Wild Type Cam and the R59A and R59K Cam Variants[a]

parameter	wild type[b]	R59A	R59K
k_{cat} ($\times 10^{-3}$ s^{-1})	7.1 ± 0.6	1.7 ± 0.1	4.8 ± 0.4
pK_a (k_{cat})	6.9	6.2 ± 0.2	6.6 ± 0.2
pK_a^I (k_{cat}/K_m^I)	6.5 ± 0.3	6.3 ± 1.4	6.5 ± 1.0
pK_a^{II} (k_{cat}/K_m^{II})	8.5 ± 0.4	9.0 ± 0.3	9.1 ± 0.3
k_{cat}/K_m^I ($\times 10^{-5}$ M^{-1} s^{-1})	17 ± 4	0.67 ± 0.53	1.3 ± 0.9
k_{cat}/K_m^{II} ($\times 10^{-5}$ M^{-1} s^{-1})	39 ± 4	8.6 ± 3.1	17.3 ± 4.8

[a] pH-independent steady-state kinetic parameters and pK_a values for CO_2 hydration were determined by fitting pH-dependent k_{cat} and k_{cat}/K_m data obtained over the pH range of 6.0−8.6 to eqs 2 and 3, as described in Materials and Methods. [b] Values from ref *23*.

DISCUSSION

Role of Arg 59 in the Thermodynamic Stability of the Cam Trimer. On the basis of the crystal structure, it was hypothesized that Arg 59 may play a role in the association of Cam monomers in the native trimer (*2*). Here we show that the R59A, -C, -H, and -K variants are trimeric and that the trimers are stable to freezing and thawing and 1.0 M GdnHCl, like the wild type. Although the freshly purified R59E, -M, and -Q variants were initially trimeric, they converted to multimeric species upon storage for several days at 4 °C or were converted to multimeric species by freezing and thawing. SEC indicated that a lower GdnHCl concentration was required to unfold the R59A and R59K variants than the wild type. These results indicate that Arg 59 contributes to the thermodynamic stability of the Cam trimer.

Importance of Arg 59 in Catalysis. The lower k_{cat} and k_{cat}/K_m values for the R59A, -C, -H, and -K variants compared to those of the wild type indicate that Arg 59 is essential for catalysis, a functional role not previously predicted for this residue. Several lines of evidence indicated that structural changes in the R59A and R59K variants were not the major contributor to the loss of activity. First, all of the variants were purified as trimers with yields similar to that of the wild type, and the CD spectra of the R59A and R59K variants were also similar to that of the wild type. Furthermore, the K_m values of the variants did not change significantly with respect to that of the wild type. Finally, GdnHCl rescued the variants in a manner indicating rescue of functionality and not structure (see below).

The k_{cat}− and k_{cat}/K_m−pH profiles for the R59K variant indicated pH-independent pK_a values similar to that of the wild type, indicating that the mechanism of the R59K variant is similar to that for the wild type. Variant R59K had 8% and all other variants <1% of the wild-type k_{cat} in the absence of GdnHCl, consistent with the importance of a positive charge at position 59. Although histidine could potentially provide the positive charge at position 59, the R59H variant had very low k_{cat} and k_{cat}/K_m values relative to those of the wild type and the R59K variant. The histidine side chain has a much lower intrinsic pK_a value of 6−7 and is shorter and less flexible than the side chains of lysine (pK_a = 10) or arginine (pK_a = 12). Thus, histidine may not have the

necessary positive charge at pH 7.5 and may not be accessible to solvent and substrates in the active site region, either reason resulting in the failure of histidine to replace arginine in catalysis.

(i) Chemical Rescue of Arg 59 Variants. Chemical rescue by positively charged guanido compounds has been observed for several enzymes containing substitutions of arginines essential for catalysis (*37*−*41*). Substantial increases were observed in k_{cat} and k_{cat}/K_m for the R59A, -C, -E, -M, and -Q variants in the presence of 100 mM GdnHCl. The ability of GdnHCl to rescue activity was confirmed by ^{18}O-labeled H_2O exchange experiments with the R59A variant.

Although direct evidence of such as a crystal structure is necessary to draw firm conclusions, several additional lines of evidence presented here are consistent with binding of rescue agents in the active site, replacing the functionality of Arg 59 and not from other nonspecific effects. First, kinetic results indicate that the GdnHCl-rescued R59A variant operates by a catalytic mechanism similar to that of the wild type. The K_m values for the GdnHCl-rescued variants were not significantly different from that of the wild type, and the k_{cat}− and k_{cat}/K_m−pH profiles for the GdnHCl-rescued R59A variant indicated pH-independent pK_a values similar to that of the wild type. Furthermore, rescue of R59A by GdnHCl occurs in a concentration-dependent manner, as indicated by both stopped-flow kinetic and ^{18}O equilibrium exchange experiments, implying that the guanido ion acts as a catalytic cofactor. The ^{18}O equilibrium exchange data also indicated that the guanidinium ion binds the R59A variant in a saturable manner, with a binding constant (K_{eff}^{GdnHCl}) of 35 mM. Second, the results suggest that GdnHCl does not simply restore a perturbed native active site conformation leading to the increased rate of catalysis. The CD spectra of the R59A variant indicate secondary structures similar to that of the wild type, independent of the presence of GdnHCl. The SEC results showed that the R59A variant is trimeric, indicating that GdnHCl does not rescue activity by converting inactive monomers into active trimers. Only positively charged guanidine and guanido compounds rescued R59A; uncharged or weakly ionized amino compounds such as urea and imidazole failed to rescue k_{cat} and k_{cat}/K_m values of the R59A variant. Third, the chemical rescue results are consistent with steric effects expected for binding of the rescue agents in the Arg 59 position.[2] The larger ethylguanidine and methylguanidine were more effective in rescuing the shorter side chain R59A variant, while the smaller guanidine was more effective in rescuing the larger side chain R59C variant than larger methylguanidine and ethylguanidine. These steric effects have also been observed in the relative ability of alkylguanido compounds to rescue arginine substitution variants of other enzymes, including the R127A variant of carboxypeptidase A (*37*), the R57G variant of ornithine transcarbamylase (*39*), and the R108Q variant of halorhodopsin (*38*). Furthermore, the k_{cat} and k_{cat}/K_m values for the five R59A, -C, -E, -M, and -Q variants exhibited an inverse dependence on the substituted side chain volume when rescued by GdnHCl.

(ii) Mechanistic Implications. Cam employs a two-step "ping-pong" catalytic mechanism similar to that of α-class carbonic anhydrases (*23*, *42*, *43*). The first step involves nucleophilic attack on a bound CO_2 molecule by zinc-coordinated OH^-, and is reflected by the catalytic efficiency, k_{cat}/K_m. The second step involves ionization of a zinc-bound water molecule for regeneration of the active site OH^- species and subsequent proton transport from the active site to external solvent or buffer which is reflected by k_{cat}. Previous studies showed one pK_a for k_{cat} and two distinct pK_a values for k_{cat}/K_m. At least one of the pK_a values for k_{cat}/K_m reflects ionization of the zinc-bound water molecule. In fast carbonic anhydrases with k_{cat} values of $>10^4$ s^{-1} (Cam, α-carbonic anhydrase II), the rate-limiting step in catalysis is proton transfer from the active site, which is assisted by a flexible proton shuttle residue located approximately 8 Å from the active site zinc ion. Glu 84 is a primary proton shuttle residue in Cam (*23*), and His 64 is a primary proton shuttle residue in the fastest α-class carbonic anhydrases (II, IV, and VII). Basic lysine and tyrosine residues more distant from the active site also function as secondary proton shuttle residues in α-class carbonic anhydrases (*44*). Substitutions of proton shuttle residues with residues having no proton transfer capability typically result in 10-fold decreases in k_{cat} and minimal changes in k_{cat}/K_m, and the variant enzymes are rescued by imidazole (*23*, *43*). The 10- to >100-fold decreases relative to those of the wild type for both k_{cat} and k_{cat}/K_m values of the R59A, -C, -E, -H, -M, and -Q variants in the absence of GdnHCl indicate that the CO_2 hydration step is significantly affected by these substitutions; however, the parallel decreases in k_{cat} and k_{cat}/K_m preclude any conclusions regarding a role for Arg 59 in the proton transfer step. The failure of imidazole to rescue R59A could be due to several reasons, including the fact that the proton transfer step is no longer rate-limiting in this variant.

The positive charge of Arg 59 may have an indirect role in catalysis. Arg 59 is the only cationic residue in the Cam active site, as the three zinc-coordinating histidines are presumably uncharged. The positive charge of Arg 59 may partially neutralize the negative charges of Asp 61, Asp 76, and Glu 62 carboxylates and the zinc-bound OH^- ion, making bicarbonate formation more thermodynamically favorable. Kiefer et al. (*45*) previously demonstrated the importance of secondary ligands in modulating the zinc affinity and the pK_a of the zinc-bound water molecule in α-class carbonic anhydrase II. The Arg 59 side chain may also influence the pK_a of the zinc-bound water molecule essential for the CO_2 hydration step through various hydrogen-bonded networks formed with Asp 61−His 81, Asp 76−His 117, active site water molecules, and Glu 62, which coordinates one of two zinc-bound water molecules. However, the large error in the fitted R59A pK_a^I value for k_{cat}/K_m may have masked any changes resulting from this substitution.

Arg 59 may also function indirectly in catalysis by binding bicarbonate. There are numerous examples of enzymes with active site arginine residues that bind carboxylate groups of substrates, including carboxypeptidase A (*6*, *46*). Transient binding of bicarbonate by Arg 59 could assist in removal of the product from the zinc ion, allowing regeneration of the active zinc−OH^- species. The bicarbonate molecule might then exit the active site through the hydrated cleft between

[2] Molecular dynamics simulations, carried out in collaboration with A. Ababou, demonstrate that, at least for the R59A variant, there is sufficient room for favorable binding of a guanidinium ion in the space formerly occupied by the Arg 59 side chain.

the monomers (T. Iverson, personal communication). Strater et al. (*10*) found that Arg 356 in aminopeptidase A binds a bicarbonate molecule that may function as a general base, facilitating proton transfer from a zinc-bound water molecule. Arg 59-bound bicarbonate could also perform a similar function in Cam. Indeed, bicarbonate enhances the rate of ^{18}O exchange between water and CO_2 in Cam (*47*). It is also possible that Arg 59 both binds bicarbonate and participates in catalysis. Dual binding and catalytic roles were deduced for Arg 11 in 4-oxalocrotonate tautomerase, based on an 88-fold decrease in k_{cat} and an 8.6-fold increase in K_m in the R11A variant (*9*). Any important mechanistic interactions between Arg 59 and bicarbonate would indicate a more complex mechanism for CO_2 hydration and bicarbonate release by Cam than that accepted for α-class carbonic anhydrases.

Summary. Two major conclusions can be made concerning the roles of Arg 59 in Cam. First, the data suggest that Arg 59 contributes to the structural integrity of both the native trimer and the active site of Cam. Although all Arg 59 variants are less stable than the wild type, the SEC characterization indicated that all variants are purified as trimers. The second, more surprising conclusion is that Arg 59 is important for catalysis. Replacement of this residue results in substantial decreases in both k_{cat} and k_{cat}/K_m, indicating that the CO_2 hydration step is affected. Arg 59 is proposed to function in the interconversion of CO_2 and HCO_3^-, product release, or both. A role for Arg 59 in the proton transfer step could not be determined but is unlikely.

ACKNOWLEDGMENT

We thank David N. Silverman, C. Robert Matthews, Tina Iverson, Brandon Doyle, Carol Fierke, and Kerry Smith for many helpful discussions and technical assistance. We also thank Abdessamad Ababou for his simulation efforts on the binding of guanidine in the R59A variant, which will be addressed in greater detail in a separate publication, and Kenneth Merz for allowing the use of the AMBER and DELPHI software, both from the Department of Chemistry, Eberly College of Science, The Pennsylvania State University.

REFERENCES

1. Parisi, G., Fornasari, M., and Echave, J. (2000) *Mol. Phylogenet. Evol. 14*, 323−334.
2. Kisker, C., Schindelin, H., Alber, B. E., Ferry, J. G., and Rees, D. C. (1996) *EMBO J. 15*, 2323−2330.
3. Iverson, T. M., Alber, B. E., Kisker, C., Ferry, J. G., and Rees, D. C. (2000) *Biochemistry 39*, 9222−9231.
4. Christianson, D. W., and Lipscomb, W. N. (1986) *Proc. Natl. Acad. Sci. U.S.A. 83*, 7568−7572.
5. Christianson, D. W., and Lipscomb, W. N. (1989) *Acc. Chem. Res. 22*, 62−69.
6. Kim, H., and Lipscomb, W. N. (1990) *Biochemistry 29*, 5546−5555.
7. Singh-Wissmann, K., Miles, R. D., Ingram-Smith, C., and Ferry, J. G. (2000) *Biochemistry 39*, 3671−3677.
8. Soundar, S., Danek, B. L., and Colman, R. F. (2000) *J. Biol. Chem. 275*, 5606−5612.
9. Harris, T. K., Czerwinski, R. M., Johnson, W. H., Jr., Legler, P. M., Abeygunawardana, C., Massiah, M. A., Stivers, J. T., Whitman, C. P., and Mildvan, A. S. (1999) *Biochemistry 38*, 12343−12357.
10. Strater, N., Sun, L., Kantrowitz, E. R., and Lipscomb, W. N. (1999) *Proc. Natl. Acad. Sci. U.S.A. 96*, 11151−11155.
11. Graber, R., Kasper, P., Malashkevich, V. N., Strop, P., Gehring, H., Jansonius, J. N., and Christen, P. (1999) *J. Biol. Chem. 274*, 31203−31208.
12. Putnam, C. D., Arvai, A. S., Bourne, Y., and Tainer, J. A. (2000) *J. Mol. Biol. 296*, 295−309.
13. Trickey, P., Wagner, M. A., Jorns, M. S., and Mathews, F. S. (1999) *Structure 7*, 331−345.
14. Erskine, P. T., Norton, E., Cooper, J. B., Lambert, R., Coker, A., Lewis, G., Spencer, P., Sarwar, M., Wood, S. P., Warren, M. J., and Shoolingin-Jordan, P. M. (1999) *Biochemistry 38*, 4266−4276.
15. Morgan, W. D., Birdsall, B., Nieto, P. M., Gargaro, A. R., and Feeney, J. (1999) *Biochemistry 38*, 2127−2134.
16. Varghese, J. N., Smith, P. W., Sollis, S. L., Blick, T. J., Sahasrabudhe, A., McKimm-Breschkin, J. L., and Colman, P. M. (1998) *Structure 6*, 735−746.
17. Jagath, J. R., Rao, N. A., and Savithri, H. S. (1997) *Biochem. J. 327*, 877−882.
18. Cronin, C. N. (1997) *Eur. J. Biochem. 247*, 1029−1037.
19. Molla, G., Porrini, D., Job, V., Motteran, L., Vegezzi, C., Campaner, S., Pilone, M. S., and Pollegioni, L. (2000) *J. Biol. Chem. 275*, 24715−24721.
20. Lindskog, S. (1997) *Pharmacol. Ther. 74*, 1−20.
21. Mallis, R. J., Poland, B. W., Chatterjee, T. K., Fisher, R. A., Darmawan, S., Honzatko, R. B., and Thomas, J. A. (2000) *FEBS Lett. 482*, 237−241.
22. Jewell, D. A., Tu, C. K., Paranawithana, S. R., Tanhauser, S. M., LoGrasso, P. V., Laipis, P. J., and Silverman, D. N. (1991) *Biochemistry 30*, 1484−1490.
23. Tripp, B. C., and Ferry, J. G. (2000) *Biochemistry 39*, 9232−9240.
24. Smith, K. S., and Ferry, J. G. (2000) *FEMS Microbiol. Rev. 24*, 335−366.
25. Strop, P., Smith, K. S., Iverson, T. M., Ferry, J. G., and Rees, D. C. (2001) *J. Biol. Chem. 276*, 10299−10305.
26. Kimber, M. S., and Pai, E. F. (2000) *EMBO J. 19*, 1407−1418.
27. Mitsuhashi, S., Mizushima, T., Yamashita, E., Yamamoto, M., Kumasaka, T., Moriyama, H., Ueki, T., Miyachi, S., and Tsukihara, T. (2000) *J. Biol. Chem. 275*, 5521−5526.
28. Alber, B. E., and Ferry, J. G. (1996) *J. Bacteriol. 178*, 3270−3274.
29. Tabor, S., and Richardson, C. C. (1985) *Proc. Natl. Acad. Sci. U.S.A. 82*, 1074−1078.
30. Sambrook, J., Fritsch, E. F., and Maniatis, T. (1989) *Molecular Cloning. A Laboratory Manual*, Cold Spring Harbor Laboratory Press, Plainview, NY.
31. Khalifah, R. G. (1971) *J. Biol. Chem. 246*, 2561−2573.
32. Silverman, D. N. (1982) *Methods Enzymol. 87*, 732−752.
33. Silverman, D. N., Tu, C., Chen, X., Tanhauser, S. M., Kresge, A. J., and Laipis, P. J. (1993) *Biochemistry 32*, 10757−10762.
34. Uversky, V. N. (1993) *Biochemistry 32*, 13288−13298.
35. Baskakov, I. V., and Bolen, D. W. (1998) *Biochemistry 37*, 18010−18017.
36. Gualfetti, P. J., Iwakura, M., Lee, J. C., Kihara, H., Bilsel, O., Zitzewitz, J. A., and Matthews, C. R. (1999) *Biochemistry 38*, 13367−13378.
37. Phillips, M. A., Hedstrom, L., and Rutter, W. J. (1992) *Protein Sci. 1*, 517−521.
38. Rudiger, M., Haupts, U., Gerwert, K., and Oesterhelt, D. (1995) *EMBO J. 14*, 1599−1606.
39. Rynkiewicz, M. J., and Seaton, B. A. (1996) *Biochemistry 35*, 16174−16179.
40. Boehlein, S. K., Walworth, E. S., Richards, N. G. J., and Schuster, S. M. (1997) *J. Biol. Chem. 272*, 12384−12392.
41. Lehoux, I. E., and Mitra, B. (2000) *Biochemistry 39*, 10055−10065.
42. Alber, B. E., Colangelo, C. M., Dong, J., Stalhandske, C. M., Baird, T. T., Tu, C., Fierke, C. A., Silverman, D. N., Scott, R. A., and Ferry, J. G. (1999) *Biochemistry 38*, 13119−13128.

43. Tu, C. K., Silverman, D. N., Forsman, C., Jonsson, B. H., and Lindskog, S. (1989) *Biochemistry 28*, 7913−7918.
44. Qian, M., Earnhardt, J. N., Wadhwa, N. R., Tu, C., Laipis, P. J., and Silverman, D. N. (1999) *Biochim. Biophys. Acta 1434*, 1−5.
45. Kiefer, L. L., Paterno, S. A., and Fierke, C. A. (1995) *J. Am. Chem. Soc. 117*, 6831−6837.
46. Kim, H., and Lipscomb, W. N. (1991) *Biochemistry 30*, 8171−8180.
47. Tu, C., Tripp, B. C., Ferry, J. G., and Silverman, D. N. (2001) *J. Am. Chem. Soc. 123*, 5861−5866.
48. Guex, N., and Peitsch, M. C. (1997) *Electrophoresis 18*, 2714−2723.
49. Zamyatin, A. A. (1972) *Prog. Biophys. Mol. Biol. 24*, 107−123.

BI010768B